Rock Mech. Rock Engng. (2002) 35 (2), 79–94

Rock Mechanics and Rock Engineering

Numerical Analysis of Blast-Induced Stress Waves in a Rock Mass with Anisotropic Continuum Damage Models Part 1: Equivalent Material Property Approach

By

H. Hao[1], **C. Wu**[2], and **Y. Zhou**[3]

[1] Department of Civil and Resource Engineering, University of Western Australia, Crawley, Australia
[2] Protective Technology Research Center, Nanyang Technological University, c\o School of CEE, Singapore
[3] Defense Science and Technology Agency, Ministry of Defense, Singapore

Summary

This paper uses the concept of anisotropic damage mechanics to analyze dynamic responses of a granite site under blasting loads. An anisotropic continuum damage model is suggested to model rock mass behavior under blasting loads. The effects of existing cracks and joints in the rock mass are considered by using equivalent rock material properties obtained from both field and laboratory test data. The anisotropic damage accumulations are simulated by continuous degradation of equivalent material stiffness and strength during loading process and are calculated using the exponential function with respect to the principal tensile strain in three directions. The suggested models are programmed and linked to an available computer program Autodyn3D through its user's subroutine capability. Stress wave propagation and damage zone in the rock mass induced by underground explosions are simulated. Numerical results of damaged area, peak particle velocity and acceleration attenuation as well as acceleration time histories and Fourier spectra are compared with those from independent field tests.

1. Introduction

Current codes and regulations to estimate stress wave intensities and damage to both nearby underground and above ground structures owing to underground blasting are usually based on some empirical or semi-empirical formulae due to the extreme complexities of the phenomena of the process in rock blasting. Different countries and group of countries apply different design manuals (NATO, 1977; Gustafsson, 1973). These empirical formulae were obtained from observations and measurements in field blast tests. They tended to overlook the physical laws governing the process in rock blasting. Since rock damage and stress wave propagation are highly dependent on material properties, data obtained from one site might not be directly used to another site. And it is very expensive to conduct

field blast tests in every site; sometimes it is impossible to carry out such tests due to the safety and environmental constraints. Thus, a reliable numerical model, validated against field measured data, is a cost-effective means of examining the highly dynamic and nonlinear process of blast-induced stress wave propagation in engineering. Developing such a numerical method has always been a challenge due to the inherently complicated properties of rock mass, blasting process, and highly nonlinear and strain rate dependent dynamic responses. It needs to properly model the explosion process, the effects of existing discontinuities in rock mass, cumulative damage of rock mass caused by blasting loads, degradation of stiffness and strength and plastic deformations of rock material.

A rock mass usually contains a lot of geological discontinuities which significantly affect the physical properties of the rock mass, and hence their dynamic responses. Because of the numerous numbers of discontinuities in a rock mass in terms of the cracks and joints, their properties such as positions, orientations, strength and stiffness, etc., are impossible to be known exactly. In practice, many researchers used equivalent rock material properties in theoretical and numerical studies of rock mass responses to either static or dynamic loads (Aimone, 1982; Zhang and Valliappan, 1990b; Schueller, 1991; Liu and Katsabanis, 1997; Zhang and Valliappan, 1998a,b). Recently, some researchers have also used discrete element method (Chen and Zhao, 1998; Hart, 1993) or block theory (Wang and Garga, 1993) to model discontinuous rock mass behavior. Because of the inherent difficulties in determining the dynamic properties of discontinuities and the complication of numerical modelling, equivalent material property approach still remains the most popular and valuable means in practice in rock engineering.

In most of the previous studies using the equivalent material properties, a rock mass was usually assumed to be isotropic (Toi and Atluri, 1990; Taylor et al., 1986; Yang et al., 1996; Liu and Katsabanis, 1997). Although isotropic assumption can give a good prediction of rock mass responses to static and dynamic loads, the calculations involved in isotropic damage state are simplified due to the scalar nature of the damage variable. And the influences of the shape, size, orientation and distribution of cracks in a rock mass, which usually result in different material properties in different directions owing to their usual predominant orientation in certain direction, cannot be captured by using approaches of the scalar damage. Such influences sometimes take an important role in controlling fracture and damage accumulation in a rock mass. Moreover, even an initially isotropic rock mass might become anisotropic owing to blasting loads because rock material strength is highly pressure sensitive, i.e., weak in tension but strong in compression. Therefore, it is meaningful to use a three-dimensional anisotropic model for rock mass in order to have more accurate estimations of its behavior under blasting loads.

The anisotropic damage model of cracked rock mass was first suggested by Kawamoto et al. (1988). They used the concept of damage mechanics to describe the cracks and joints in a rock mass as its initial damage. Zhang and Valliappan (1990a) also modeled the cracks and joints in a rock mass as its anisotropic initial damage, and they further used the statistical theory to derive a statistical initial damage in the rock mass. They included the statistical initial damage in estimating

the slope stability of the rock mass under static loads (Zhang and Valliappan, 1990b). In these studies, the rock responses to static loads and the initial damage were all modeled as anisotropic. A continuum anisotropic damage model for brittle material under low strain rate dynamic loading is developed by Yazdchi et al. (1996). However, few papers can be found to use the anisotropic damage theory to analyze the behavior of a rock mass under high strain rate dynamic loads, such as blasting loads.

In this paper, an anistropic damage model based on the hypothesis of stress working equivalence is presented to model rock damage resulting from blasting-induced stress waves. The effects of existing cracks and joints are considered by using equivalent material properties. The anisotropic damage accumulation is simulated by the continuous degradation of equivalent material stiffness and strength during the loading process and is calculated using an exponential function with respect to the principal tensile strain. A modified Drucker-Prager model and a modified linear equation of state as proposed in a previous paper (Hao et al., 1998) are used to model the strength and stiffness degradation of the pressure sensitive rock material. The anisotropic cumulative damage in the model is determined by material properties, namely the threshold strain ε_{cri} and constants α_i and β_i that will be discussed later.

The present anisotropic damage model has been implemented in a transient, dynamic finite difference and finite element code Autodyn3D (1997) as its user defined subroutines. Numerical results obtained will be compared with the data measured in independent field blasting tests (Zhao et al., 1997). It shows that the model can well predict the blasting-induced stress wave in the rock mass. Numerically simulated peak particle velocity and acceleration attenuation as well as acceleration time histories and Fourier spectra all agree favorably with the field measured data. It demonstrates that the anisotropic damage model results in more accurate prediction on accelerations of the stress wave than the results obtained earlier by the authors with isotropic assumption (Wu et al., 1999).

2. Dynamic Response Equations

The equation of motion for an anisotropic damaged body can be written using the variational principles as (Valliappan, 1991)

$$[M]\{a\} + [C]\{v\} + [K(D_1(t), D_2(t), D_3(t))]\{u\} = \{P(t)\}, \tag{1}$$

where

$$[M] = \int_v \rho [N]^T [N]\, dV \tag{2}$$

is the mass matrix for damaged rock mass; ρ and $[N]$ represent the mass density and shape-function matrix; $\{a\}$ is the system nodal acceleration vector; $[C]$ is the viscous damping matrix; $\{v\}$ is the system nodal velocity vector; $[K(D_1(t), D_2(t), D_3(t))]$ is the time-dependent stiffness matrix defined as

$$[K(D_1(t), D_2(t), D_3(t))] = \int_V [B]^T [T]^T [\tilde{E}][T][B]\, dV, \tag{3}$$

$\{u\}$ is the system nodal displacement vector and $\{P(t)\}$ is the system nodal force vector due to surface and body forces

$$[P(t)] = \int_s [N]^T [Q(t)]\, ds + \int_V [N]^T [F(t)]\, dV, \tag{4}$$

in which $[T]$ is the coordinate transformation matrix, $[B]$ is the strain displacement matrix, and $[\tilde{E}]$ is the damaged constitutive matrix in the orthotropic damage space, and $D_i(t),\ i = 1, 2, 3$ are time-dependent damage scalar in the three directions.

By assuming the complementary elastic energy of the damage state equal to that of the undamaged state, the elastic constitutive relation pertinent to the anisotropic damage model in 3-D space is (Yazdchi et al., 1996)

$$\{\tilde{\sigma}\} = [\tilde{E}]\{\tilde{\varepsilon}\}, \tag{5}$$

where

$$[S^*] = [S^*_{ij}] = [\tilde{E}]^{-1} = \begin{bmatrix} \frac{1}{E^*_1} & -\frac{v^*_{21}}{E^*_2} & -\frac{v^*_{31}}{E^*_3} & 0 & 0 & 0 \\ -\frac{v^*_{12}}{E^*_1} & \frac{1}{E^*_2} & -\frac{v^*_{32}}{E^*_3} & 0 & 0 & 0 \\ -\frac{v^*_{13}}{E^*_1} & -\frac{v^*_{23}}{E^*_2} & \frac{1}{E^*_3} & 0 & 0 & 0 \\ 0 & 0 & 0 & \frac{1}{2G^*_{23}} & 0 & 0 \\ 0 & 0 & 0 & 0 & \frac{1}{2G^*_{31}} & 0 \\ 0 & 0 & 0 & 0 & 0 & \frac{1}{2G^*_{12}} \end{bmatrix}, \tag{6}$$

in which

$$E^*_i = E(1 - D_i(t))^2 \quad i = 1, 2, 3, \tag{7}$$

$$v^*_{ij} = v_{ij} \frac{1 - D_i(t)}{1 - D_j(t)} \quad i, j = 1, 2, 3, \tag{8}$$

$$G^*_{ij} = G_{ij} \frac{(1 - D_i(t))^2 (1 - D_j(t))^2}{(1 - D_i(t))^2 + (1 - D_j(t))^2} \quad i, j = 1, 2, 3, \tag{9}$$

and E, v_{ij} and G_{ij} are undamaged elastic modulus, Poisson's ratio, and shear modulus, respectively; E^*_i, v^*_{ij} and G^*_{ij} are corresponding damaged material parameters.

With a suitable damage evolution equation, constitutive law and damage model, Eq. (1) can be solved by the dynamic Lagrangian finite element and finite difference program, such as Autodyn3D.

3. Anisotropic Damage Model

Under intense dynamic loading, damage will be initiated and grow in a rock mass. It is reasonable to assume that cumulative damage is accumulated over time and

is irreversible. There are a few definitions of evolutionary damage law in literature. For the damage evolution of low strain rate, two major damage evolution criteria (Yazdchi et al., 1996) have been proposed for different kinds of materials, the first one is a power function of tensile stress and the other one is based on damage strain energy release rate. For damage evolution of high strain rate, cumulative damage scalar evolution of rock masses under blasting loads was considered as function of the damaged Poisson's ratio (Taylor, 1986), or extensional volumetric strain (Yang et al., 1996), or volumetric tensile strain (Liu and Katsabanis, 1997). In a previous study with isotropic assumption, it was proven that the definition based on the volumetric tensile strain yielded fairly good results (Hao et al., 1998). In the present study, the damage scalar evolution of rock mass under explosion loads based on the volumetric tensile strain is extended to the case of anisotropic damage. The corresponding damage evolution equation in the anisotropic principal axis is defined as

$$D_i(t) = 1 - e^{-C_i V_0} \quad i = 1, 2, 3, \tag{10}$$

where V_0 is a unit volume; C_i is crack density in the i-th direction, which can be calculated by

$$C_i = \begin{cases} \alpha_i(\varepsilon_i - \varepsilon_{cri})^{\beta_i} t & \varepsilon_i > \varepsilon_{cri} \\ 0 & \varepsilon_i \le \varepsilon_{cri} \end{cases} \quad i = 1, 2, 3, \tag{11}$$

where α_i and β_i are material constants in the i-th anisotropic principal axis; ε_i is the principal strain in the i-th direction; and ε_{cri} is the corresponding principal critical tensile strain.

The material parameters, namely α_i, β_i, and ε_{cri}, need be determined from the dynamic fracture properties of the rock mass. Ideally, they should be determined by triaxial tensile test data. In reality, however, it is very difficult to carry out triaxial tensile tests. Since a rock mass under stress wave propagation always experiences both tensile and compressive strains simultaneously in its three principal directions, and rock damage is usually controlled by tensile strain, in the present study, uniaxial tensile test results are used to approximately model rock failure. Thus, the critical tensile strain ε_{cri} can easily be determined from the uniaxial static tensile test results,

$$\varepsilon_{cri} = \sigma_{sti}/\bar{E}_i \quad i = 1, 2, 3, \tag{12}$$

where σ_{sti} is the static tensile strength and $\bar{E}_i = E(1 - D_i^s)^2$ is the equivalent elastic modulus in the i-th direction, in which D_i^s is the equivalent initial damage D_i^s in three directions.

If the tensile strain and crack density in the i-th direction corresponding to the fracture stress are denoted by ε_{fi} and C_{dfi}, respectively, from Eq. (11), it has

$$C_{dfi} = \alpha_i(\varepsilon_{fi} - \varepsilon_{cri})^{\beta_i}(t_i - t_{ci}) \quad i = 1, 2, 3, \tag{13}$$

where t_i is the total time to reach the fracture stress,

$$t_i = \frac{\varepsilon_{fi}}{\dot{\varepsilon}_i} \quad i = 1, 2, 3, \tag{14}$$

and t_{ci} is the time duration needed for the tensile strain ε_{fi} to reach the critical value ε_{cri}, and

$$t_{ci} = \frac{\varepsilon_{cri}}{\dot{\varepsilon}_i} \quad i = 1, 2, 3, \tag{15}$$

where $\dot{\varepsilon}_i$ is the strain rate of uniaxial tension. Submit Eqs. (14) and Eq. (15) to Eq. (13), to obtain

$$C_{dfi} = \alpha_i (t_i \dot{\varepsilon}_i - t_{ci} \dot{\varepsilon}_i)^{\beta_i} (t_i - t_{ci}) \quad i = 1, 2, 3. \tag{16}$$

The time beyond critical time t_{ci} required for stress to reach the fracture stress is then

$$t_i - t_{ci} = \left(\frac{C_{dfi}}{\alpha_i} \right)^{1/(1+\beta_i)} \dot{\varepsilon}_i^{-(\beta_i/(1+\beta_i))} \quad i = 1, 2, 3. \tag{17}$$

The relationship between the fracture stress σ_{fi} and strain ε_i is

$$\varepsilon_i = \sigma_{fi} / \bar{E}_i (1 - D_{fi})^2 \quad i = 1, 2, 3, \tag{18}$$

where D_{fi} is the cumulative damage corresponding to the fracture stress in the i-th direction, which can be estimated from Eq. (10) by replacing C_i by C_{dfi}.

Submit Eqs. (12) and (18) to Eq. (13), to obtain

$$C_{dfi} = \alpha_i \left(\frac{\sigma_{fi}}{\bar{E}_i (1 - D_{fi})^2} - \frac{\sigma_{sti}}{\bar{E}_i} \right)^{\beta_i} (t_i - t_{ci}) \quad i = 1, 2, 3. \tag{19}$$

Then, the fracture stress σ_{fi} at a certain strain rate in uniaxial tensile state can be obtained as,

$$\sigma_{fi} = (1 - D_{fi})^2 \sigma_{sti} + \bar{E}_i (1 - D_{fi})^2 \left(\frac{C_{dfi}}{\alpha_i} \right)^{1/(1+\beta_i)} \dot{\varepsilon}_i^{1/(1+\beta_i)} \quad i = 1, 2, 3. \tag{20}$$

From Eq. (20), we have

$$\alpha_i = \left(\frac{(1 - D_{fi})^2 \bar{E}_i}{\sigma_{fi} - (1 - D_{fi})^2 \sigma_{sti}} \right)^{1+\beta_i} C_{dfi} \dot{\varepsilon}_i. \tag{21}$$

As for β_i, since fracture stress for many brittle material such as rock depends on the cube root of the strain rate, it can be taken as equal to 2 (Liu and Katsabanis, 1997; Hao et al., 1998).

In the model by Grady and Kipp (1980) the minimum cumulative damage value is set to be equal to 0.2, because it provided a "reasonable match" between calculation and experiment. While in the model by Thorne et al. (1990), another damage parameter, F, is used with a minimum value equal to 0.693. The physical meaning for minimum damage values used in the mentioned models is fuzzy. According to the numerical investigations of rock blasting by Liu and Katsabanis (1997), the isotropic damage value is about 0.632 when the dynamic tensile stress reaches the dynamic failure stress. In this study, $D_{fi} = 0.632$ is assumed when the rock mass is considered failed, implying $C_{dfi} = 1$ in Eq. (10), then the parameter α_i

can be determined from Eq. (21) at any given tensile strain rate. ε_{cri} is calculated by Eq. (12). Based on the laboratory test data of granite at the site under consideration (Soil and Foundation Ltd., 1996), the elastic modulus of the undamaged rock material is estimated to be 93.87 GPa (Wu et al., 1999). On the other hand, the geological investigation on site shows that many discontinuities exist in the rock mass. Based on the orientations, spacing, normalized size of cracks and number of cracks in the rock mass, a three-dimensional geometric model has been derived to estimate the anisotropic initial damage in a previous study (Wu et al. 2001). Using the geometric model, it is found that the equivalent initial damage D_i^s in three directions, namely X, Y, and Z as indicated in Fig. 1, or directions 1, 2 and 3, are 0.162, 0.124, and 0.222 (Wu et al., 2001). Thus the equivalent elastic moduli for the granite in the three directions can be determined by Eq. (7). They

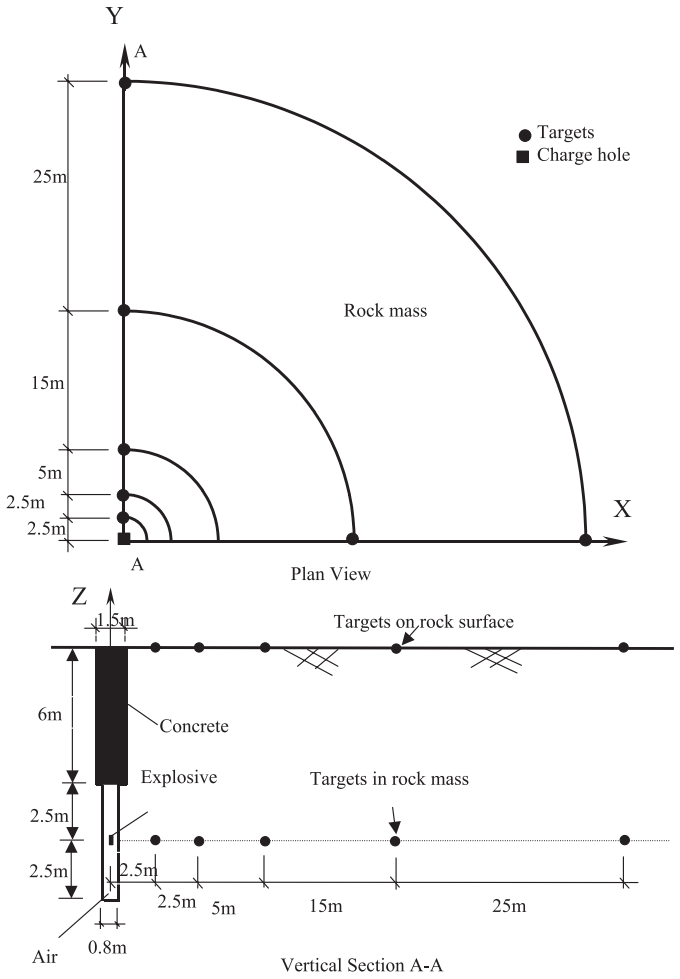

Fig. 1. Field layout and vertical section of small scale tests (not to scale)

are $\bar{E}_1 = 65.92$ GPa, $\bar{E}_2 = 69.10$ GPa, and $\bar{E}_3 = 56.82$ GPa. Based on Eq. (12), the equivalent critical tensile strain ε_{cr1}, ε_{cr2} and ε_{cr3} are then calculated as 0.265×10^{-3}, 0.253×10^{-3} and 0.307×10^{-3}, respectively. Using the above data, the constant α_1, α_2 and α_3 are calculated by Eq. (21) as $\alpha_1 = 5.85 \times 10^{10}$, $\alpha_2 = 6.74 \times 10^{10}$, and $\alpha_3 = 3.75 \times 10^{10}$.

4. Numerical Implementation

The constitutive law and anisotropic damage model described in the previous sections together with the modified Drucker-Prager strength criterion and modified linear equation of state (Hao et al., 1998) are implemented into Autodyn3D program as user defined subroutines. In numerical calculation, the cumulative damage in each element can be determined based on Eq. (10), thus, making it possible to model both damage propagation and damage growth. During loading, the damage of each element is accumulated for every time increment. The element stiffness matrix at the end of the previous time step is used to calculate the system stiffness matrix for the current time step. The state of strain and stress in each element is obtained and used in damage evolution law to update the damage tensor components, and hence the element stiffness matrix and element strength at every time step. Consistent with the damage-based continuum mechanics approach used here, the element failure is defined by a minimum criterion

$$D_i(t) = 1 - \exp(-\alpha_i(\varepsilon_i - \varepsilon_{cri})^{\beta_i} tV) \geq D_{fi} \quad i = 1, 2, 3, \tag{22}$$

where $D_i(t)$ is anisotropic cumulative damage in the i-th direction under explosion loading and D_{fi} is the respective critical damage value, and V is the volume of the element under consideration. The damage calculated at each time step are compared to its critical value D_{fi}. When Eq. (22) is satisfied for a specific element, the element is considered to have failed and it is assumed to be capable of supporting only the hydrostatic compressive stresses.

5. Field Test Layout and Numerical Model

The above model with modified Autodyn3D program is used to simulate a series of field blasting tests carried out at the granite site under consideration. The field layout, as shown in Fig. 1, consists of a step charge hole with a total depth of 11 m. The upper 6 m of the charge hole has a diameter of 1.5 m and the bottom 5 m has a diameter of 0.8 m. More than 100 gages, including accelerometers, pressure sensors and strains gages were used for different measurements. The measuring points were placed along two lines on rock surface. In the X direction, they are placed at 25 m and 50 m; and in the Y direction they are placed at 2.5 m, 5 m, 10 m, 25 m, and 50 m distance from the charge hole center. The measurement holes were also drilled to place accelerometers at the same level of the explosive (8.5 m below rock surface) in the Y direction with a distance of 2.5 m, 5 m, 10 m, 25 m, and 50 m from the charge hole center. After accelerometers were placed in the positions, the measurement holes were filled with grouting materials with similar

properties as the granite mass. At each point, two pieces of piezoelectric accelerometers were placed to record the radial (horizontal) and vertical accelerations. More detailed descriptions of the test set up and implementation can be found in a report by Zhao et al. (1997).

Eight tests were carried out with the equivalent TNT charge weights ranging from 5 kg to 50 kg and loading densities from 2 kg/m^3 to 20 kg/m^3 (explosive weight divided by charge hole volume). In order to simulate a contained explosion, the charge chamber (bottom 5 m of the charge hole) was covered by a 50 mm thick steel plate and 8 concrete blocks with a total weight of 15 t to prevent any uplifting. Explosive used is PETN, which has an equivalent charge weight ratio of 1.41 to TNT. In each test, explosive was placed at the center of the charge chamber on a wooden stand. The recorded data were used to derive empirical attenuation relations for peak particle velocity and peak particle acceleration. The best fitted empirical attenuation relations are given in the following (Zhao et al., 1997):

$$\mathrm{PPA} = 1928.2(R/Q^{1/3})^{-1.4531}\ (\mathrm{g}) \tag{23}$$

$$\mathrm{PPV} = 0.396(R/Q^{1/3})^{-1.1455}\ (\mathrm{m/s}), \tag{24}$$

where R is distance in meter measured from the charge center; Q is equivalent TNT charge weight in kilogram. It should be noted that the above empirical attenuation equations were derived by using the data obtained from the tests with loading densities varying from 2 kg/m^3 to 20 kg/m^3. This is because the peak values of stress waves do not vary significantly in this range of loading densities. This observation is consistent with other field test data and the loading density effect is usually neglected when it is less than 50 kg/m^3 (Odello, 1998).

In numerical modelling, air and equivalent explosive TNT are simulated by Euler processor and are assumed to satisfy the equation of state (EOS) of ideal gas and EOS of JWL (Jones-Wilkens-Lee), respectively. Rock material is modeled by the modified orthotropic linear EOS and simulated by Lagrange processor (Hao et al., 1998; Wu et al., 1999). The whole domain, including rock, air and TNT, is assumed to be symmetric in the X and Y directions. Thus only one quarter of the rock mass is modeled in the numerical model. Transmitting boundary is used to reduce reflection of stress wave from the numerical boundaries. The material constants of the rock mass obtained from site investigation are used in numerical simulation, while standard constants of air and TNT are from the Autodyn3D material library. These include Poisson's ratio of the granite $\nu = 0.16$; averaged mass density of granite 2650 kg/m^3, air mass density $\rho = 1.225$ kg/m^3; air initial internal energy $En = 2.068 \times 10^5$ kJ/kg; and ideal air constant $\gamma = 1.4$. The shear modulus of the rock mass depends on the elastic modulus E_i and Poisson's ratio ν, and also degrades with the damage variable D_i. In the present study, initial Poisson's ratio is still assumed to be isotropic. It should be noted that viscous damping effect is neglected in the numerical simulation as its influence on high velocity explosion-type responses is insignificant. It should also be noted that the continuum damage mechanics theory is employed in the current study to define the rock mass damage. The rock mass is modeled as a continuum solid subjected to impulsive

load induced by explosion. Damage to the rock mass is caused by stress wave propagation through the rock mass that generates strains larger than the threshold strain as defined in Eqs. (10) and (11). Damage due to the penetration/explosion of the explosive gas into the existing fractures is not considered. Such damage was not considered by other researchers in their study of rock damage to explosive load (Taylor et al., 1986; Yang et al., 1996; Liu and Katsabanis, 1997). However, numerical results obtained by those researchers as well as in the present study indicate that modeling only the damage induced by stress wave propagation can give reasonable prediction of rock mass response to blasting load.

6. Numerical Results and Analysis

The proposed numerical model is used to simulate the above field blasting test in the granite mass. Figure 2 shows comparison of the calculated peak particle velocities (PPV) and the calculated peak particle accelerations (PPA) with isotropic and anisotropic damage model in the rock mass (free field) at different scaled distances in the Y direction. The corresponding best fitted curves of the field measured data

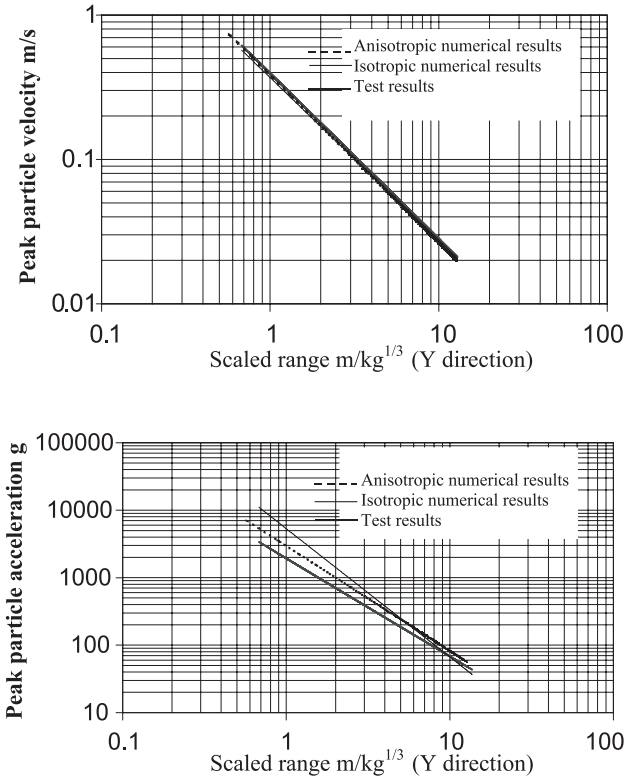

Fig. 2. Comparison of attenuation of PPV and PPA in the Y direction

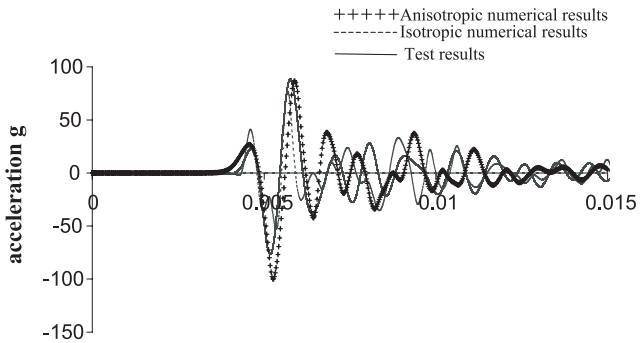

Fig. 3. Comparison of horizontal acceleration time histories (radial direction) in the rock mass at 25 m from the charge hole in the Y direction (charge weight 50 kg)

in the Y direction are also plotted in the figure. As can be seen, numerical results agree well with the field measured data for PPV. Compared to the PPV calculated in the Y direction with isotropic assumption (Wu et al., 1999), the present results are similar, if not better, implying the PPV stress wave can be well predicted by using either isotropic or anisotropic damage model. It is noteworthy that improvement on the accuracy of PPA in the Y direction is achieved if anisotropic damage model is used as compared with those calculated by using the isotropic model (Wu et al., 1999). The largest error between the simulated PPA and field measured data differ by about 2 times in the present study, while the largest difference between the measured PPA and PPA simulated without considering anisotropic damage is 3.5 times (Wu et al., 1999).

Figure 3 shows the comparison of the recorded and simulated acceleration time histories (in radial direction) in the rock mass in the Y direction at 25 m from the charge hole when charge weight is 50 kg. It shows that the wave form and peak value of the simulated stress wave with anisotropic damage agree better with those of the recorded motion than those obtained from isotropic damage model. Figure 4 shows comparison of the corresponding Fourier spectra of the simulated and recorded acceleration time histories. It shows that, the spectrum of the simulated acceleration time history obtained by anisotropic damage model is more accurate than that obtained by isotropic model at frequencies higher than 1500 Hz. It indicates that the isotropic model fails to simulate the attenuation of high frequency energy in stress wave by rock mass anisotropy.

Figure 5 shows the recorded and simulated acceleration time histories on the rock surface at 50 m from the charge hole in the X and the Y directions. Reasonably good matches are observed again. As shown, the PPA recorded in the Y direction is slightly larger than that recorded in the X direction. Figure 6 shows comparison of their Fourier spectra. It shows that the dominant frequencies of the recorded and simulated acceleration time histories are similar. It also shows that the principal frequency of the stress wave in the X direction is smaller than that in the Y direction because more discontinuities exist in the X direction which cause high frequency energy to attenuate more rapidly. The amplitudes of the Fourier

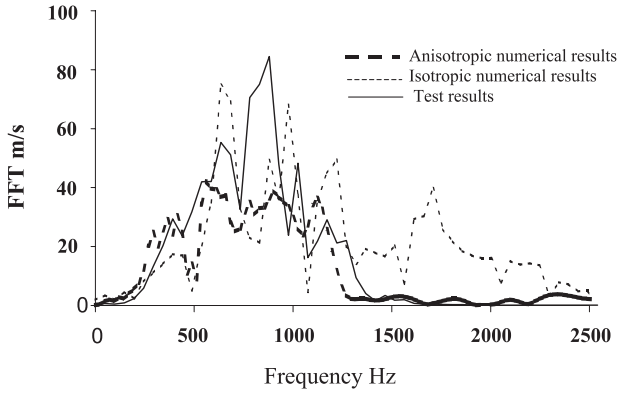

Fig. 4. Comparison of FFT of horizontal acceleration time histories (radial direction) in the rock mass at 25 m from the charge hole in the Y direction (charge weight 50 kg)

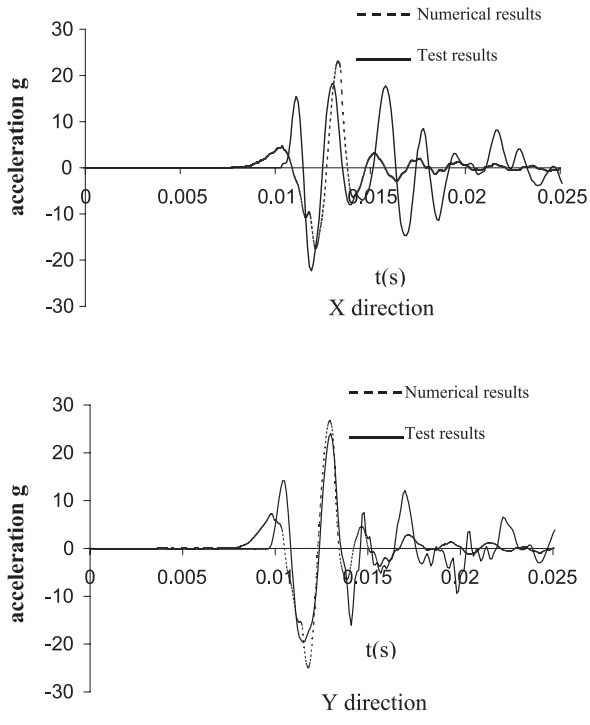

Fig. 5. Comparison of horizontal acceleration time histories (radial direction) on the rock surface at 50 m from the charge hole in the X and Y directions (charge weight 50 kg)

spectra of the simulated stress wave on rock surface are higher than those of the recorded motion. This is reasonable because equivalent material property approach does not consider vigorously the effects of existing cracks in the rock mass, which will cause certain wave reflection, thus smaller Fourier spectra amplitudes.

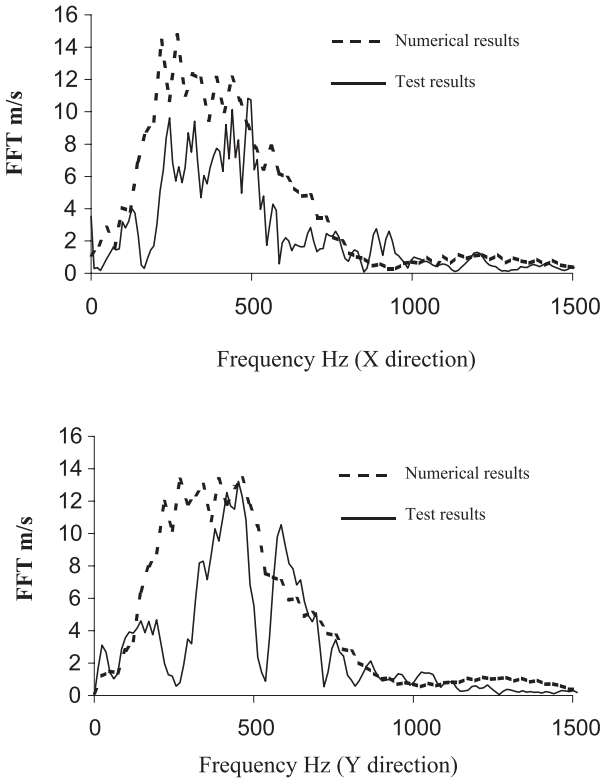

Fig. 6. Comparison of FFT of horizontal acceleration time histories (radial direction) in the rock mass at 50 m from the charge hole in the X and Y directions (charge weight 50 kg)

The field observation of some falling crashed rock blocks in the charge hole after explosion indicated that some damage was created around the charge hole when the charge weight was 50 kg with a loading density of 20 kg/m^3 (Zhao et al., 1997).

Figure 7 shows the calculated damage zone around the charge hole in the rock mass when charge weight is 50 kg. The damage variable at any particular point is defined as $D = \max D_i(t)$, where $D_i(t)$ is determined by Eq. (10). When D is larger than, say, 0.63 as suggested by Liu and Katsabanis (1997), the rock mass is considered failed. As shown in the figure, the intensive damage zone ($D > 0.63$) is about 1.22 m in the X direction and 1.07 m in the Y direction deep into the rock mass. This damage level indicates excessive cracks in the rock mass and possible falling of rock blocks. These results are consistent with the field observations that shows falling of rock blocks after 50 kg detonation in the charge hole, although the exact depth of the crack extension in the rock mass of the field test is unknown. To more accurately calibrate the damage zone simulated by the present numerical model, further field blast tests are necessary. It should also be noted that the damage zone in the Y direction is smaller than that in the X direction. This is also due to the pre-existing damage in the X direction.

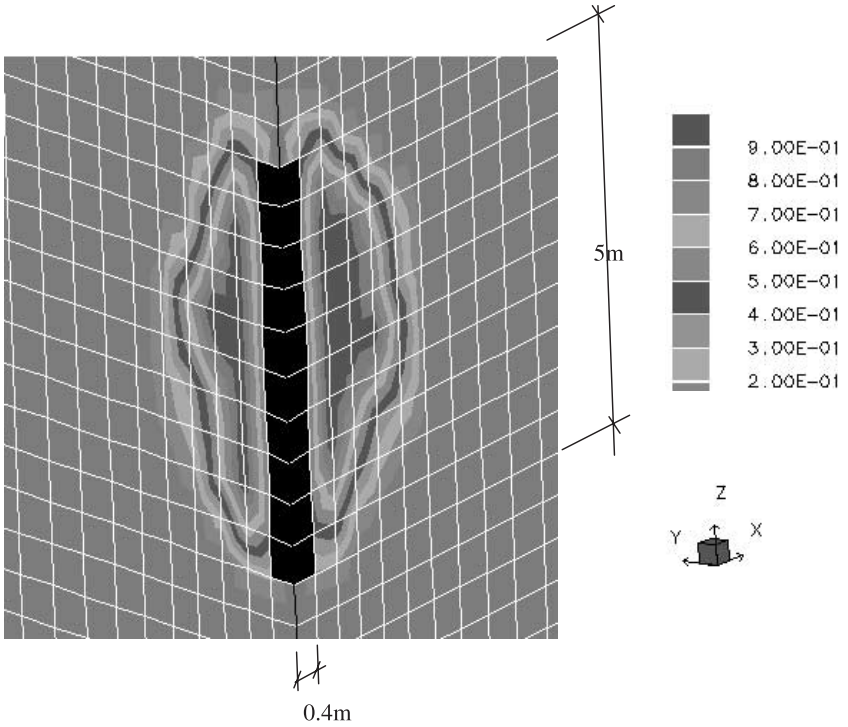

Fig. 7. Distribution of damage variable D around the charge hole (charge weight 50 kg)

7. Conclusions

Based on the theory of continuum damage mechanics, computational methods were developed for the analysis of dynamic responses of rock mass under blasting loads. An anisotropic damage model has been presented in the present study. The model is capable of describing the rate-dependent non-linear behavior of rock masses. Damage evolution based on exponential function of principal tensile strain has been used here to calculate the cumulative damage. Using Autodyn3D together with the proposed anisotropic damage model, an independently conducted field test has been numerically simulated. It was found that the peak particle velocity, peak particle acceleration, acceleration time history and Fourier spectra of acceleration all agreed favorably well with test results. It was also demonstrated that numerical results based on anisotropic damage model are more accurate than those based on isotropic damage model in predicting underground blasting-induced stress wave accelerations. The validity of the proposed model for a rock mass under blasting loads has been proved. Using anisotropic model, non-isotropic damage zone and stress wave propagation in a rock mass can be simulated.

References

Aimone, C. T. (1982): Three-dimensional wave propagation model of full-scale rock fragmentation. Ph.D. Thesis, Northwestern University, Evanston, IL.

Autodyn3D (1997): AUTODYN User Manual, Revision 3.0. Century Dynamics, San Ramon, CA.

Chen, S. G., Zhao, J. (1998): A study on UDEC modelling of blast wave propagation in jointed rock mass. Int. J. Rock Mech. Min. Sci. 35, 93–99.

Grady, D. E., Kipp, M. E. (1980): Continuum modelling of explosive fracture in oil shale. Int. J. Rock Mech. Min. Sci. Geomech. Abstr. 17, 147–157.

Gustafsson, R. (1973): Swedish blasting technique. SPI, Gothenburg, Sweden.

Hao, H., Ma, G. W., Zhou, Y. X. (1998): Numerical simulation of underground explosions. Fragblast, Int. J. Blasting Fragment. 2, 383–395.

Hart, R. D. (1993): An introduction to distinct element modelling for rock engineering. In: Hudson, J. A. (ed.) Comprehensive rock engineering, vol. 2. Pergamon Press, Oxford, 245–261.

Kawamoto, T., Ichikawa, Y., Kyoya, T. (1988): Deformation and fracturing behavoiur of discontinuous rock mass and damage mechanics theory. Int. J. Numer. Anal. Methods Geomech. 12, 1–30.

Liu, L., Katsabanis, P. D. (1997): Development of a continuum damage model for blasting analysis. Int. J. Rock Mech. Min. Sci. 34, 217–231.

NATO (1997): Manual on NATO safety principles for the storage of ammunition and explosives. In document: AC/258-D/258, Brussels, Belgium.

Odello, R. J. (1998): Origins and implications of underground explosives storage regulations. Int. Symposium of Transient Loading and Response of Structures, Trondheim, Norway.

Schueller, C. T. (1991): Structural dynamics. Springer, Berlin Heidelberg New York Tokyo.

Soil and Foundation Ltd. (1996): Seismic survey and site investigation works at Mandai for Lands and Estates Organization. Vol. I, Site investigation. Ministry of Defence, Singapore.

Taylor, L. M., Chen, E. P., Kuszmaul, J. S. (1986): Micro-crack induced damage accumulation in brittle rock under dynamic loading. Computer Meth. Appl. Mech. Eng. 55, 301–320.

Thorne, B. J., Hommert, P. J., Brown, B. (1990): Experimental and computational investigation of the fundamental mechanisms of cratering. 3rd Int. Symposium on Rock Fragmentation by Blasting, Brisbane, Australia, 412–423.

Toi, Y., Atluri, S. N. (1990): Finite element analysis of static and dynamic fracture of brittle micro-cracking solids. Int. J. Plasticity 6, 389–414.

Valliappan, S. (1991): Analysis of anisotropic damage mechanics problems. In: Atluri, S. N. et al. (eds.), Proc. Int. Conf. Computational Engineering Science, Melbourne, Australia, 1142–1147.

Wang, B. L., Garga, V. K. (1993): A numerical method of modelling large displacements of jointed rocks. Part I: Fundamentals. Canadian Geotech. J. 30, 96–108.

Wu, C., Hao, H., Zhou, Y. X. (1999): Dynamic response analysis of rock mass with stochastic properties subjected to explosive loads. Fragblast, Int. J. Blasting Fragment. 3, 137–153.

Wu, C., Hao, H., Zhao, J., Zhou, Y. X. (2001): Statistical analysis of anisotropic damage of the Bukit Timah granite. Rock Mech. Rock Engng. 39(1), 23–38.

Yang, R., Bawden, W. F., Katsabanis, P. D. (1996): A new constitutive model for blast damage. Int. J. Rock Mech. Min. Sci. Geomech. Abstr. 33, 245–254.

Yazdchi, M., Valliappan, S., Zhang, W. (1996): A continuum model for dynamic damage evolution of anisotropic brittle materials. Int. J. Numer. Methods Eng. 39, 1555–1583.

Zhang, W., Valliappan, S. (1990a): Analysis of random anisotropic damage mechanics problems of rock mass, Part I: Probabilistic analysis. Rock Mech. Rock Engng. 23, 91–112.

Zhang, W., Valliappan, S. (1990b): Analysis of random anisotropic damage mechanics problems of rock mass, Part II: Statistical estimation. Rock Mech. Rock Engng. 23, 241–259.

Zhang, W., Valliappan, S. (1998a): Continuum damage mechanics theory and application, Part I: Theory. Int. J. Damage Mechanics 7, 250–273.

Zhang, W., Valliappan, S. (1998b): Continuum damage mechanics theory and application, Part II: Application. Int. J. Damage Mechanics 7, 274–297.

Zhao, J., Wu, Y. K., Cai, J. G., Chen, S. G., Zhao, Y. H. (1997): Small-scale ground shock tests at the Mandai Quarry. Technical Report to Lands and Estates Organization, Ministry of Defense, Singapore.

Authors' address: Prof. Dr. Hong Hao, Department of Civil and Resource Engineering, University of Western Australia, 35 Stirling Highway, Crawley, WA 6003, Australia.